Theory of indirect hyperfine interactions of oxygen-aluminum defects in ionic crystals

F. J. Adrian and A. N. Jette

Milton S. Eisenhower Research Center, Applied Physics Laboratory, The Johns Hopkins University,
Johns Hopkins Road, Laurel, Maryland 20707

J. M. Spaeth

Fachbereich Physik, Universität Paderborn, Warburger Strasse 100A D-4790 Paderborn, Federal Republic of Germany

Aluminum hyperfine interactions of the $Al^{3+}-O^-$-trapped-hole center in a number of oxides containing Al ions either as a constituent (Al_2O_3:Mg^{2+}, Na β-alumina) or as an impurity (GeO_2, SiO_2) are analyzed with use of a semiempirical model of the exchange polarization mechanism of transferred hyperfine interactions. The theory quantitatively predicts the observed strong dependence of the negative isotropic hyperfine constant on the O^--Al^{3+} distance and, from estimates of the electrostatic-crystal-field energy at O^-, indicates a reasonable outward expansion ($\sim 10\%$) of the Al^{3+} ions next to the O^- hole center. The theory also accounts well for the observation that the anisotropic hyperfine constants in these centers vary only slightly despite the large variation in the corresponding isotropic splittings.

I. INTRODUCTION

Trapped hole centers have been investigated by electron-spin resonance (ESR) and electron-nuclear double resonance (ENDOR) in a number of oxides containing Al^{3+} ions either as a constituent like in Al_2O_3 or as an impurity.[1-5] The hole is trapped at an O^{2-} anion forming O^- and hyperfine interactions with one or several neighboring Al^{3+} ions are measured. These hyperfine (hf) interactions usually showed two distinct peculiarities: The isotropic hf constant (hfc), denoted A, was negative and the anisotropic hfc, denoted $B_{||}$, was much smaller than the value one would expect from classical dipole-dipole interaction between the unpaired electron (hole) and the magnetic Al nucleus. Strictly speaking, from the experiments it could only be said that A and $B_{||}$ had opposite signs, but $B_{||}$ is always assumed to be positive because of the classical dipole-dipole interaction. The common electronic configuration for these centers is that the Al^{3+} neighbor is in a nodal plane of the unpaired O^- p orbital, so that there is zero overlap between it and the Al^{3+} ion core and, consequently, no direct transferred positive hf interaction. An indirect mechanism, exchange polarization, is well known and has been applied in a number of cases,[6-11] of which the V_K center[8] is an example similar to the centers of interest here; it presents great computational difficulties because of the large number of excited-state configurations needed to describe the exchange polarization. In analyzing the ESR spectra of these oxygen-aluminum defect centers and determining their structures, we shall use, therefore, a semiempirical perturbation method of calculating these indirect hfc's in which average excitation energies are introduced to enable summation over complete sets of the excited states. This method[11] of calculating indirect hfc's will be extended to cover defects in ionic crystals as contrasted with ionic molecular radicals, and the contribution of the indirect

mechanism to anisotropic, as well as, isotropic hfc's will be discussed.

The theory is applied to O^--Al^{3+} centers in Na β-alumina, GeO_2 and SiO_2, Al_2O_3:Mg^{2+} (Refs. 1–4) and will be found to explain the experimental data of these rather different centers in different crystals quite well. It predicts the strong dependence of the isotropic hyperfine constant on the O^--Al^{3+} distance quantitatively, and also accounts for the fact, that the anisotropic hyperfine constants are nearly independent of O^--Al^{3+} distance, having nearly the same low value in all systems. The theory can be used to determine rather precisely the relaxed O^--Al^{3+} distance if a value for the electrostatic-crystal-field energy at O^- is known. The results show that the increase in O^--Al^{3+} distance due to the charge repulsion is much smaller ($\sim 10\%$) than the values derived from the classical dipole-dipole interaction alone, from which it was concluded that the bond lengths would increase by up to approximately 40%.[2,4]

II. THEORY

The zeroth-order valence-bond (VB) wave function of the oxygen-aluminum system of Fig. 1 is

$$\Psi_0 = \mathscr{A}\,\psi_{Al}(1s)\overline{\psi_{Al}(1s)}\psi_{Al}(2s)\overline{\psi_{Al}(2s)} \times \cdots$$

$$\times \psi_O(2s)\overline{\psi_O(2s)}\psi_O(2p_z)\overline{\psi_O(2p_z)}\psi_O(2p_y)\,, \qquad (1)$$

where $\mathscr{A}$ is the antisymmetrization and renormalization operator, and the ψ's are one-electron Hartree-Fock atomic orbitals (AO's) centered on aluminum (subscript Al) and oxygen (subscript O) nuclei, respectively, and the dots (i.e., $\cdots$) denote orbitals that are not explicitly written out (e.g., the Al p orbitals) in the interest of saving space. $\overline{\psi}$ is the AO of opposing spin relative to ψ. Thus, the total wave function is an antisymmetric product of all the one-electron AO's centered on the oxygen and aluminum nu-
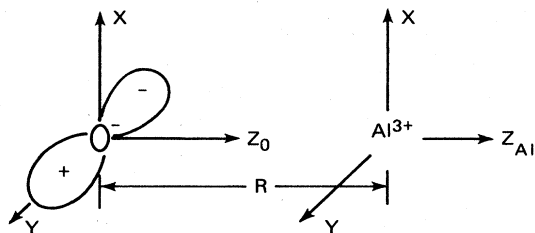
FIG. 1. Coordinate convention for the aluminum-oxygen centers where the unpaired electron is in a π orbital $(2p_y)$ localized on the oxygen.

clei. Since the unpaired electron is an oxygen $2p_y$ orbital, the spin density evaluated with this wave function at the aluminum nucleus is zero.

There is a small spin density in the nodal plane of the $2p_y$ unpaired electron, however, due to the spin polarization of the doubly occupied AO's by the exchange interactions between the unpaired electron and the electrons in these AO's with the same spin as the unpaired electron. Of these AO's the $2s$ and $2p_z$ functions of the anion are the most important since they have the largest overlap with the aluminum nucleus. As discussed previously,[11] the unpaired $2p_y$ oxygen electron also exchange polarizes the paired AO's localized on the aluminum nucleus, but the contribution of these terms to the transferred aluminum hfc is quite small because the excitation energies for exciting the metal AO's are very much larger than the oxygen excitation energies. Thus, the important excitations to consider are $2s \rightarrow m$ and $2p \rightarrow n$ excitations of the oxygen anion. The first-order wave function in the exchange perturbation is accordingly,

$$\Psi_1 = \Psi_0 + \sum_n{}' \frac{\langle \psi_O(2p_y)\psi_O(n) \,|\, (e^2/r_{12}) \,|\, \psi_O(2p_z)\psi_O(2p_y)\rangle}{(\epsilon_n - \epsilon_{2p})_O} \mathscr{A}[\cdots \psi_{Al}(2s)\overline{\psi_{Al}(2s)} \cdots \psi_O(n)\overline{\psi_O(2p_z)}\psi_O(2p_y)]$$

$$+ \sum_m{}' \frac{\langle \psi_O(2p_y)\psi_O(m) \,|\, (e^2/r_{12}) \,|\, \psi_O(2s)\psi_O(2p_y)\rangle}{(\epsilon_m - \epsilon_{2s})_O}$$

$$\times \mathscr{A}[\cdots \psi_{Al}(2s)\overline{\psi_{Al}(2s)} \cdots \psi_O(m)\overline{\psi_O(2s)}\psi_O(2p_z)\overline{\psi_O(2p_z)}\psi_O(2p_y)] , \tag{2}$$

where the primes on the summations indicate that $n = 2p_z$ or $m = 2s$ is to be excluded from the sums. For the two-electron integrals, the following convention is followed:

$$\langle \psi_O^I(1)\psi_O^{II}(2) \,|\, (e^2/r_{12}) \,|\, \psi_O^{III}(1)\psi_O^{IV}(2)\rangle ,$$

where the first function in the "bra" or "ket" pertains to electron No. 1 while the second is a function of electron No. 2.

A. ISOTROPIC hfc

The transferred isotropic hfc is given by the expectation value of the operator

$$H_F = \frac{16\pi}{3} \frac{\mu_O\mu_{Al}}{I_{Al}} \sum_i \delta(\mathbf{r}_i - \mathbf{R}_{Al})\mathbf{I}_{Al}\cdot\mathbf{S}_i \tag{3}$$

with the VB function, in Eq. (2), where μ_O is the Bohr magneton, and μ_{Al} and I_{Al} are the magnetic moment and spin of the aluminum nucleus. The sum is over all the electrons of the system. The important terms for the aluminum isotropic hfc (A), i.e., to first order in the exchange perturbation, are

$$A = 2\sum_n{}' \left[\sum_{i=1}^{2}\sum_{j=1}^{2} \langle \psi_O(2p_z) \,|\, \psi_{Al}(is)\rangle\langle \psi_{Al}(is) \,|\, H_F \,|\, \psi_{Al}(js)\rangle\langle \psi_{Al}(js) \,|\, \psi_O(n)\rangle \right.$$

$$\left. \times \frac{\langle \psi_O(2p_y)\psi_O(n) \,|\, (e^2/r_{12}) \,|\, \psi_O(2p_z)\psi_O(2p_y)\rangle}{(\epsilon_n - \epsilon_{2p})_O} \right]$$

$$+ 2\sum_m{}' \left[\sum_{i=1}^{2}\sum_{j=1}^{2} \langle \psi_O(2s) \,|\, \psi_{Al}(is)\rangle\langle \psi_{Al}(is) \,|\, H_F \,|\, \psi_{Al}(js)\rangle\langle \psi_{Al}(js) \,|\, \psi_O(m)\rangle \right.$$

$$\left. \times \frac{\langle \psi_O(2p_y)\psi_O(m) \,|\, (e^2/r_{12}) \,|\, \psi_O(2s)\psi_O(2p_y)\rangle}{(\epsilon_m - \epsilon_{2s})_O} \right] . \tag{4}$$

As denoted by the prime in the summation, Eq. (4) involves sums over all orbitals which are unoccupied in the ground state. To perform these sums, an average excitation energy is introduced in order to remove the energy denominators from the summations. That is $(\epsilon_n - \epsilon_{2p})_O$ and $(\epsilon_m - \epsilon_{2s})_O$ are replaced by the positive constants $\overline{[\epsilon(2p \rightarrow np)]}_O$ and

$\overline{[\epsilon(2s \rightarrow ns)]}_O$, respectively.

Now, if we complete the sums in Eq. (4) by adding in the ground-state-occupied orbitals and subtracting them separately and then use the average-energy approximation and the fact that the orbitals of a given atom form a complete set, Eq. (4) may be reduced to an expression involving only the ground state. Those terms resulting from applying the completeness theorem to the sum over all orbitals contain products of overlap and two-center exchange integrals. As discussed in detail previously,[11] a typical such term resulting from summing over the complete set of oxygen orbitals contains the matrix element product

$$\langle \psi_O(2p_z) \mid \psi_{Al}(is) \rangle \langle \psi_O(2p_y)\psi_{Al}(js) \mid (1/r_{12}) \mid \psi_O(2p_z)\psi_O(2p_y) \rangle \ .$$

These terms are considerably smaller (15% or less) than the corresponding terms involving the ground-state-occupied orbitals which were introduced to complete the sums in Eq. (4). The ground-state product corresponding to the example just given is

$$\langle \psi_O(2p_z) \mid \psi_{Al}(is) \rangle \langle \psi_O(2p_y)\psi_O(2p_z) \mid (1/r_{12}) \mid \psi_O(2p_z)\psi_O(2p_y) \rangle \langle \psi_{Al}(js) \mid \psi_O(2p_z) \rangle \ .$$

Thus, for simplicity in this approximate calculation, only the latter terms are considered in obtaining

$$
\begin{aligned}
A = \frac{16\pi}{3} \frac{\mu_O \mu_{Al}}{I_{Al}} & \left[\frac{-2}{[\epsilon(2p \rightarrow np)]_O} \left[\langle \psi_O(2p_y)\psi_O(2p_z) \mid (e^2/r_{12}) \mid \psi_O(2p_z)\psi_O(2p_y) \rangle \right. \right. \\
& \left. \times \sum_{i=1}^{2} \sum_{j=1}^{2} \langle \psi_O(2p_z) \mid \psi_{Al}(is) \rangle \langle \psi_{Al}(is) \mid \delta(\mathbf{r}-\mathbf{R}_{Al}) \mid \psi_{Al}(js) \rangle \langle \psi_{Al}(js) \mid \psi_O(2p_z) \rangle \right] \\
& - \frac{2}{[\epsilon(2s \rightarrow ns)]_O} \left[\langle \psi_O(2p_y)\psi_O(2s) \mid (e^2/r_{12}) \mid \psi_O(2s)\psi_O(2p_y) \rangle \right. \\
& \left. \left. \times \sum_{i=1}^{2} \sum_{j=1}^{2} \langle \psi_O(2s) \mid \psi_{Al}(is) \rangle \langle \psi_{Al}(is) \mid \delta(\mathbf{r}-\mathbf{R}_{Al}) \mid \psi_{Al}(js) \rangle \langle \psi_{Al}(js) \mid \psi_O(2s) \rangle \right] \right] \ .
\end{aligned}
$$

$$\text{(5)}$$

Actually, there should also be contributions from the $\psi_O(1s)$ spin polarization of the shell in Eq. (5), but these were neglected since both $\langle \psi_O(1s) \mid \psi_{Al}(js) \rangle$ and $\langle \psi_O(2p_y)\psi_O(1s) \mid (e^2/r_{12}) \mid \psi_O(2s)\psi_O(2p_y) \rangle$ are smaller than the corresponding matrix elements of the oxygen $2s$ electron by an order of magnitude, and the excitation energy of the O $1s$ electron is extremely large.

There are two contributions to the average excitation energies; namely, the electrostatic contribution, since the O^- nucleus is at a center of positive charge, and the average of the energies required to excite the O^- $2s$ and $2p$ electrons in the free O^- anion. Since the missing electron occupied a $2p_y$ orbital, the electrostatic contribution is approximately the interaction of a positively charged $2p_y$ hole with the electron that is being excited, i.e.

$$V_{2p_y}(i) = \int \int \mid \psi_O(2p_y;r_2) \mid^2 \frac{e^2}{r_{12}} \mid \psi_O(i;r_1) \mid^2 d\tau_1 d\tau_2 \ , \tag{6}$$

where $i = 2s$ or $2p_z$. The average energy to excite the $2s$ and $2p$ electrons is taken as three-fourths their respective expectation values of the Hartree-Fock operator which by Koopmans theorem is the ionization energy for that electron. Thus,

$$\overline{\epsilon(i \rightarrow n)} = V_{2p_y}(i) - 3\epsilon_i/4 \ , \tag{7}$$

which quantities are tabulated in Table I along with the

quantities

$$A_{is,js} = \frac{16\pi}{3} \frac{\mu_O \mu_{Al}}{I_{Al}} \langle \psi_{Al}(is) \mid \delta(\mathbf{r}-\mathbf{R}_{Al}) \mid \psi_{Al}(js) \rangle \tag{8}$$

and

$$K_{kl}^{ij} = \langle \psi_O(i)\psi_O(j) \mid (e^2/r_{12}) \mid \psi_O(k)\psi_O(l) \rangle \ . \tag{9}$$

The K_{kl}^{ij} were calculated using the Hartree-Fock AO's of Clementi and Roetti.[12] The necessary integrals are tabulated in Table II along with the isotropic hfc as a function of the Al-O distance. The isotropic hfc A, according to Eq. (5), follows very well an exponential law with distance in the range considered for the $O^- $-$Al^{3+}$ distance, between 3 and 4 Bohr radii (a_0). To facilitate comparison with experimental data, A can be represented with the same precision as the values in Table II by the following expression:

$$
A = - \left[\frac{2.592 \times 10^3}{[\epsilon(2p \rightarrow np)]_O} \exp(-1.6113R) \right.
$$
$$
\left. + \frac{56.114 \times 10^3}{[\epsilon(2s \rightarrow ns)]_O} \exp(-2.7317R) \right] \text{MHz} \ , \tag{10}
$$

where R is the distance in a.u. (a_0) and the excitation energies $\bar{\epsilon}$ are in hartrees (H).

TABLE I. Parameters appearing in Eqs. (5), (11), and (13) for the transferred hfc's of aluminum. 1 H $\approx$ 27.2 eV.

$K^{2p_y 2s}_{2s 2p_y} = 0.140\,21$ H

$\epsilon_{2s} = -0.813\,27$ H

$K^{2p_y 2p_z}_{2p_z 2p_y} = 0.033\,41$ H

$\epsilon_{2p} = -0.129\,26$ H

$A_{1s,1s} = 7.616 \times 10^5$ MHz

$[\epsilon(2s \rightarrow ns)]_0 = 1.315$ H

$A_{1s,2s} = -1.982 \times 10^5$ MHz

$[\epsilon(2p \rightarrow np)]_0 = 0.725$ H

$A_{2s,2s} = 0.516 \times 10^5$ MHz

$4\mu_0 \mu_{Al}/I_{Al} = 277.72$ MHz a.u.^{3}

$V_{2p_y}(2s) = 0.705$ H

$\left\langle \psi_{Al}(2p_y) \left| \dfrac{C_0^2(\theta_{Al})}{r_{Al}^3} \right| \psi_{Al}(2p_y) \right\rangle = -7.057\,76$ a.u.$^{-3}$

$V_{2p_y}(2p_z) = 0.628$ H

$\left\langle \psi_{Al}(2p_z) \left| \dfrac{C_0^2(\theta_{Al})}{r_{Al}^3} \right| \psi_{Al}(2p_z) \right\rangle = 14.115\,52$ a.u.$^{-3}$

TABLE II. Two center integrals appearing in Eq. (5), and the isotropic transferred aluminum hfc.

R (a.u.)	$\langle \psi_{Al}(1s) \mid \psi_O(2s) \rangle$	$\langle \psi_{Al}(2s) \mid \psi_O(2s) \rangle$	$\langle \psi_{Al}(1s) \mid \psi_O(2p_z) \rangle$	$\langle \psi_{Al}(2s) \mid \psi_O(2p_z) \rangle$	A (MHz)
3.00	0.004622	0.050497	0.015125	0.135515	-40.2
3.17	0.003594	0.039899	0.012966	0.117304	-29.1
3.20	0.003438	0.038266	0.012622	0.114367	-27.5
3.40	0.002554	0.028911	0.010582	0.096688	-18.9
3.60	0.001895	0.021786	0.008910	0.081918	-13.1
3.80	0.001404	0.016375	0.007533	0.069571	-9.2

TABLE III. Two-center integrals appearing in Eqs. (12) and (14).

R (a.u.)	3.00	3.17	3.20	3.40	3.60	3.80
$\left\langle \psi_O(2p_y) \left\| \dfrac{C_0^2(\theta_{Al})}{r_{Al}^3} \right\| \psi_O(2p_y) \right\rangle$	0.024 63	0.021 71	0.021 24	0.018 41	0.016 03	0.014 26
$\left\langle \psi_O(2s) \left\| \dfrac{C_0^2(\theta_{Al})}{r_{Al}^3} \right\| \psi_O(2s) \right\rangle$	0.035 54	0.030 50	0.029 70	0.025 00	0.021 17	0.018 10
$\left\langle \psi_O(2p_z) \left\| \dfrac{C_0^2(\theta_{Al})}{r_{Al}^3} \right\| \psi_O(2p_z) \right\rangle$	0.045 60	0.039 08	0.038 05	0.031 95	0.027 00	0.022 95
$\left\langle \psi_{Al}(2p_y) \left\| \dfrac{C_0^2(\theta_{Al})}{r_{Al}^3} \right\| \psi_O(2p_y) \right\rangle$	$-0.013\,83$	$-0.011\,32$	$-0.010\,94$	$-0.008\,71$	$-0.006\,99$	$-0.005\,63$
$\langle \psi_O(2p_y) \mid \psi_{Al}(2p_y) \rangle$	0.030 43	0.025 02	0.024 17	0.019 30	0.015 49	0.012 49
$\langle \psi_O(2p_z) \mid \psi_{Al}(2p_z) \rangle$	$-0.075\,72$	$-0.065\,53$	$-0.063\,86$	$-0.053\,73$	$-0.045\,17$	$-0.037\,98$
$\langle \psi_O(2s) \mid \psi_{Al}(2p_z) \rangle$	$-0.047\,21$	$-0.037\,97$	$-0.036\,52$	$-0.028\,11$	$-0.021\,55$	$-0.016\,46$
$M^{2p_y 2p_z}_{2p_z 2p_y}$	0.001 48	0.001 26	0.001 22	0.001 02	0.000 85	0.000 72
$M^{2p_y 2s}_{2s 2p_y}$	0.004 18	0.003 64	0.003 56	0.003 05	0.002 62	0.002 27
$N^{2p_y 2p_z}_{2p_z 2p_y}$	$-0.000\,64$	$-0.000\,45$	$-0.000\,43$	$-0.000\,28$	$-0.000\,19$	$-0.000\,12$
$N^{2p_y 2p_z}_{2s 2p_y}$	$-0.000\,89$	$-0.000\,62$	$-0.000\,58$	$-0.000\,38$	$-0.000\,25$	$-0.000\,16$

B. Anisotropic hfc

The anisotropic hfc, $B_{||}$, is the component of the expectation value of the electron spin-nuclear spin dipole-dipole interaction, H_D, along the oxygen-aluminum axis. For simplicity, only an axially symmetric hf tensor is treated here. Unlike the isotropic hfc considered above, both the zeroth-order VB function (1) and the polarization terms of the first-order perturbed VB function in Eq. (2) contribute to $B_{||}$. Denoting these two contributions as the direct contribution, $B^D_{||}$, and the polarization contribution, $B^P_{||}$, respectively, the anisotropic hfc is given by

$$B_{||} = B^D_{||} + B^P_{||} , \qquad (11)$$

where

$$B_{||}^D = \frac{4\mu_O\mu_{Al}}{I_{Al}} \left[\left\langle \psi_O(2p_y) \left| \frac{C_0^2(\theta_{Al})}{r_{Al}^3} \right| \psi_O(2p_y) \right\rangle - 2\langle \psi_O(2p_y) | \psi_{Al}(2p_y) \rangle \right.$$

$$\times \left\langle \psi_{Al}(2p_y) \left| \frac{C_0^2(\theta_{Al})}{r_{Al}^3} \right| \psi_O(2p_y) \right\rangle + \langle \psi_O(2p_y) | \psi_{Al}(2p_y) \rangle$$

$$\left. \times \left\langle \psi_{Al}(2p_y) \left| \frac{C_0^2(\theta_{Al})}{r_{Al}^3} \right| \psi_{Al}(2p_y) \right\rangle \langle \psi_{Al}(2p_y) | \psi_O(2p_y) \rangle \right] . \tag{12}$$

Procedures similar to those used to derive the isotropic hfc but considering the overlap of the oxygen orbitals with the aluminum $2p$ orbitals give

$$B_{||}^P = \frac{4\mu_O\mu_{Al}}{I_{Al}} \left[2\sum_n{}' \left[\left\langle \psi_O(2p_z) \left| \frac{C_0^2(\theta_{Al})}{r_{Al}^3} \right| \psi_O(n) \right\rangle - 2\langle \psi_O(2p_z) | \psi_{Al}(2p_z) \rangle \left\langle \psi_{Al}(2p_z) \left| \frac{C_0^2(\theta_{Al})}{r_{Al}^3} \right| \psi_O(n) \right\rangle \right. \right.$$

$$\left. + \langle \psi_O(2p_z) | \psi_{Al}(2p_z) \rangle \left\langle \psi_{Al}(2p_z) \left| \frac{C_0^2(\theta_{Al})}{r_{Al}^3} \right| \psi_{Al}(2p_z) \right\rangle \langle \psi_{Al}(2p_z) | \psi_O(n) \rangle \right]$$

$$\times \frac{\langle \psi_O(2p_y)\psi_O(n) | (e^2/r_{12}) | \psi_O(2p_z)\psi_O(2p_y) \rangle}{(\epsilon_n - \epsilon_{2p})_O}$$

$$+ 2\sum_m{}' \left[\left\langle \psi_O(2s) \left| \frac{C_0^2(\theta_{Al})}{r_{Al}^3} \right| \psi_O(m) \right\rangle - 2\langle \psi_O(2s) | \psi_{Al}(2p_z) \rangle \left\langle \psi_{Al}(2p_z) \left| \frac{C_0^2(\theta_{Al})}{r_{Al}^3} \right| \psi_O(m) \right\rangle \right.$$

$$\left. + \langle \psi_O(2s) | \psi_{Al}(2p_z) \rangle \left\langle \psi_{Al}(2p_z) \left| \frac{C_0^2(\theta_{Al})}{r_{Al}^3} \right| \psi_{Al}(2p_z) \right\rangle \langle \psi_{Al}(2p_z) | \psi_O(m) \rangle \right]$$

$$\left. \times \frac{\langle \psi_O(2p_y)\psi_O(m) | (e^2/r_{12}) | \psi_O(2s)\psi_O(2p_y) \rangle}{(\epsilon_m - \epsilon_{2s})_O} \right] . \tag{13}$$

In the above equations, $C_0^2(\theta_{Al})$ is the reduced spherical harmonic defined by

$$C_m^l(\theta,\phi) \equiv [4\pi/(2l+1)]^{1/2} Y_l^m(\theta,\phi) .$$

The sums over n and m are again evaluated by introducing the average excitation energies, completing the set by adding to the sums the excluded $n = 2p_z$ and $m = 2s$ terms and finally subtracting these terms.

The resulting expression involves a number of terms that roughly cancel in pairs. Even so, however, the expression for $B_{||}^P$ is more complicated than for A, of Eq. (5), because the isotropic counterparts of a number of the terms in Eq. (13) were either zero or negligible due to the spherical symmetry and the infinitely short-ranged character of the isotropic hf operator. The nonnegligible terms of this expression are

$$B_{||}^P = \frac{4\mu_O\mu_{Al}}{I_{Al}} \left\{ \frac{2}{[\epsilon(2p \to np)]_O} \left[M_{2p_z2p_y}^{2p_y2p_z} + \langle \psi_O(2p_z) | \psi_{Al}(2p_z) \rangle \left\langle \psi_{Al}(2p_z) \left| \frac{C_0^2(\theta_{Al})}{r_{Al}^3} \right| \psi_{Al}(2p_z) \right\rangle N_{2p_z2p_y}^{2p_y2p_z} \right. \right.$$

$$- K_{2p_z2p_y}^{2p_y2p_z} \left[\left\langle \psi_O(2p_z) \left| \frac{C_0^2(\theta_{Al})}{r_{Al}^3} \right| \psi_O(2p_z) \right\rangle + \langle \psi_O(2p_z) | \psi_{Al}(2p_z) \rangle \right.$$

$$\left. \left. \times \left\langle \psi_{Al}(2p_z) \left| \frac{C_0^2(\theta_{Al})}{r_{Al}^3} \right| \psi_{Al}(2p_z) \right\rangle \langle \psi_{Al}(2p_z) | \psi_O(2p_z) \rangle \right] \right]$$

$$+ \frac{2}{\epsilon(2s \to ns)} \left[M_{2s2p_y}^{2p_y2s} + \langle \psi_O(2s) | \psi_{Al}(2p_z) \rangle \left\langle \psi_{Al}(2p_z) \left| \frac{C_0^2(\theta_{Al})}{r_{Al}^3} \right| \psi_{Al}(2p_z) \right\rangle \right.$$

$$\times N_{2s2p_y}^{2p_y2p_z} - K_{2s2p_y}^{2p_y2s} \left[\left\langle \psi_O(2s) \left| \frac{C_0^2(\theta_{Al})}{r_{Al}^3} \right| \psi_O(2s) \right\rangle \right.$$

$$+ \langle \psi_O(2s) | \psi_{Al}(2p_z) \rangle \left\langle \psi_{Al}(2p_z) \left| \frac{C_0^2(\theta_{Al})}{r_{Al}^3} \right| \psi_{Al}(2p_z) \right\rangle$$

$$\left. \left. \left. \times \langle \psi_{Al}(2p_z) | \psi_O(2s) \rangle \right] \right] \right\} , \tag{14}$$

TABLE IV. Anisotropic hfc as a function of oxygen-aluminum distance.

R (a.u.)	$B_{\parallel}^{0}$ (MHz)	$B_{\parallel}^{P}$ (MHz)	$B_{\parallel}$ (MHz)
3.00	5.26	−3.53	1.73
3.17	4.96	−2.60	2.36
3.20	4.90	−2.46	2.44
3.40	4.47	−1.71	2.76
3.60	4.04	−1.19	2.85
3.80	3.69	−0.83	2.86

where the two-electron exchange-type terms are defined by

$$M_{kl}^{ij} \equiv \left\langle \psi_O(i)\psi_O(j) \left| \frac{C_0^2(\theta_{Al,2})}{r_{Al,2}^3} \frac{e^2}{r_{12}} \right| \psi_O(k)\psi_O(l) \right\rangle \quad (15)$$

and

$$N_{kl}^{ij} \equiv \left\langle \psi_O(i)\psi_{Al}(j) \left| (e^2/r_{12}) \right| \psi_O(k)\psi_O(l) \right\rangle . \quad (16)$$

The various parameters and matrix elements are tabulated in Tables I and III. The anisotropic hfc is given in Table IV as a function of the aluminum-oxygen distance.

The polarization part of $B_{\parallel}$, has an exponential dependence on distance in the $3-4a_0$ range of O^--Al^{3+} distances, analogous to that found for the isotropic hfc. The expression, which also can facilitate comparison of theory and experiment, is

$$B_{\parallel}^{P} = - \left[\frac{84.7 e^{-1.426R}}{[\epsilon(2p \to np)]_O} + \frac{2086 e^{-2.237R}}{[\epsilon(2s \to ns)]_O} \right] . \quad (17)$$

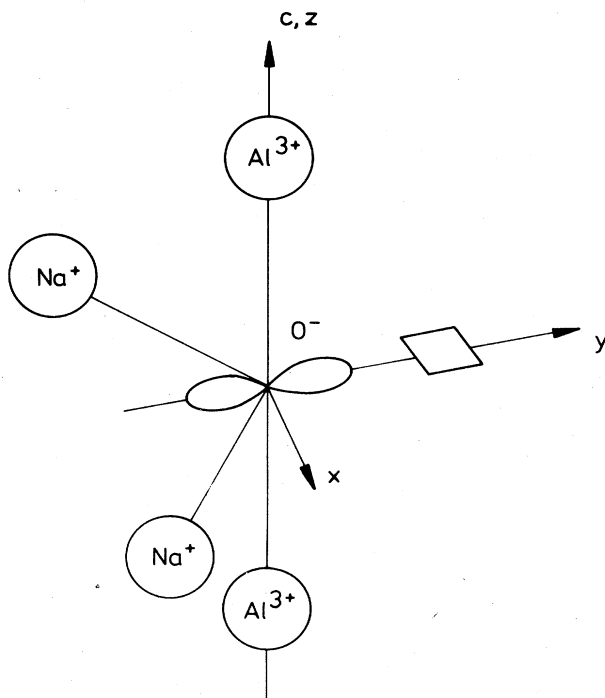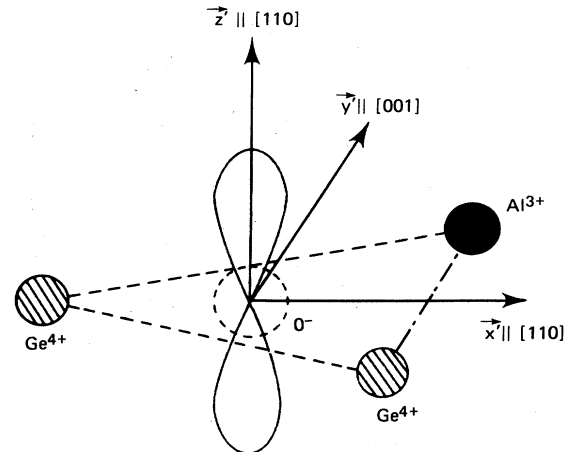FIG. 3. Model of the O^--Al^{3+} center in GeO_2 (after Ref. 2).

III. COMPARISON WITH EXPERIMENTAL RESULTS AND DISCUSSION

Figures 2—5 show the models for several O^--Al^{3+} centers which have been studied by ESR or ENDOR and where negative isotropic hfc's and small anisotropic hfc's were found. In all cases the Al^{3+} ion was in the nodal plane of the unpaired O^- $2p_y$ orbital. In Na β-alumina the orientation of the $2p_y$ orbital is determined by a Na^+ vacancy in the mirror plane[1] (Fig. 2). In GeO_2 (Ref. 2) and SiO_2 (Ref. 3), Al^{3+} is incorporated as an impurity and the hole is trapped at a nearby O^{2-} ion. In GeO_2 (Fig. 3) the hole is perpendicular to the plane spanned by Al^{3+}-Ge^{4+}-Ge^{4+} while in SiO_2 it is thought to be perpendicular to the plane spanned by Al^{3+}-O(3)-Si(3) (see Fig. 4). In Al_2O_3 doped with Mg^{2+} it was established by ENDOR[4] that the hole interacts with two Al^{3+} ions in the first shell and one Al^{3+} ion in the second shell and that one Al^{3+} neighbor is missing in the second shell. This is in agreement with an earlier g-factor analysis.[13,14] The Al^{3+} va-
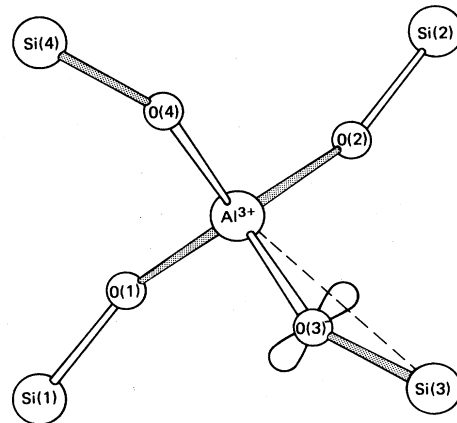
FIG. 2. Model of the O^--Al^{3+} center in Na β-alumina (after Ref. 1).

FIG. 4. Model of the O^--Al^{3+} center in SiO_2 (after Ref. 3). Shorter Si-O bonds are indicated by shading.

TABLE V. Comparison of theoretical and experimental hfc's for several O^--Al^{3+} centers.

| Center | | Experiment | | | | Theory | | |
	$R_0(a_0)$	A (MHz)	$B_{\parallel}$ (MHz)	V_{2p_y} (H)	$A(R_0)$ (MHz)	R/R_0	$B_{\parallel}$ (MHz)
O^- in Na-β-alumina (Ref. 1)	3.17	-23.1	1.6	0.368	-43.7	1.11	2.2
$(Al)^0$ in GeO_2 (Ref. 2)	3.54	-12.5	1.86	0.706	-13.5	1.01	2.9
$(AlO_4)^0$ in SiO_2 (Ref. 3)	3.40	-16.2	2.10	0.368	-28.6	1.09	2.4
O^- in Al_2O_3:Mg^{2+} (Ref. 4)	3.75	-7.3	2.18	0.559[a]	-11.1	1.06	2.7
	3.45	-14.2	2.06		-19.0	1.05	2.7
	3.30	-19.0	2.00		-25.2	1.05	2.6
				0.283[b]	-18.4	1.14	2.3
					-31.4	1.13	2.3
					-41.1	1.13	2.2

[a]Assuming Al^{3+} vacancy.

[b]Assuming Mg^{2+} in Al^{3+} vacancy.

cancy is most probably filled by a Mg^{2+}, but this, however, could not be conclusively determined from the analysis of the ENDOR data.[4] The oxygen is assumed to be in the plane spanned by two first-shell and one second-shell Al^{3+} neighbors and the unpaired p orbital is perpendicular to that plane. (See Fig. 5). The experimental hfc's of the four O^--Al^{3+} defect centers are given in Table V. Except for O^- in Na β-alumina, the hf tensors were found not to be fully axially symmetric. However, in view of the approximate nature of the theory only the "axial" part $B_{\parallel}=B_{zz}=2b$ of the anisotropic tensor is listed and discussed. In general, one must consider also $B_{xx}=-b+b'$ and $B_{yy}=-b-b'$, b' representing the deviation from axial symmetry. b' is, however, small for the centers considered here.

Figure 6 shows that the isotropic hfc, A, varies exponentially with the distance between O^- and Al^{3+}. The solid line was calculated with the parameters given in Tables I and II. Also plotted are the experimental isotropic hfc's for the four centers of Table V, taking the O^--

Al^{3+} distance to be the regular $O^{2-}-Al^{3+}$ distance, R_0, for an undistorted lattice. In the case of O^- in Al_2O_3:Mg^{2+} the site of O^- within the triangle spanned by the two first-shells and one second-shell Al^{3+} neighbors is not known. Using the slope of $1n\,|A|$ versus O^--Al^{3+} distance from Eq. (10) and V_{2p_y} from Table I (solid line in Fig. 6) one can find a particular site within the undistorted Al^{3+} triangle from which the distances to the three Al^{3+} corners are such that the experimental isotropic hfc's approximately follow the exponential law with the theoretical slope in the semilog plot. These distances are
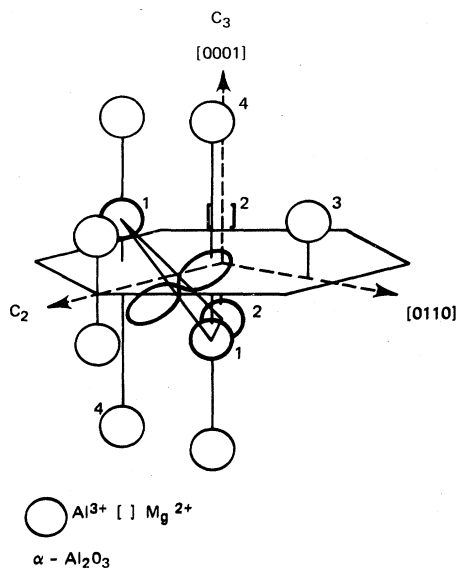

FIG. 5. Model of the O^--Al^{3+} center in α-Al_2O_3:Mg^{2+} (after Ref. 4).
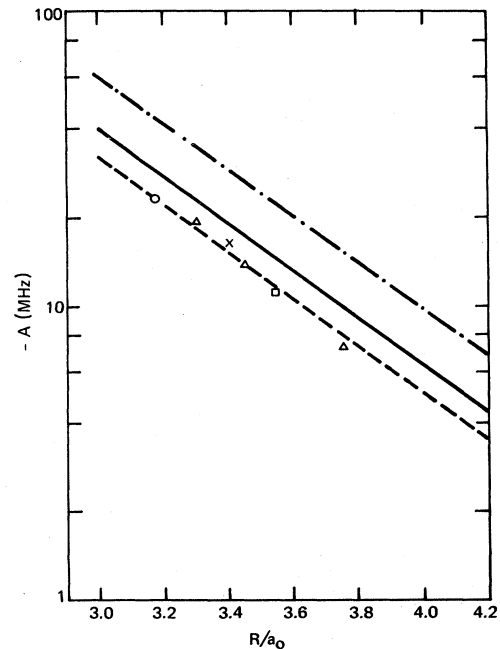

FIG. 6. Semilog plot of the isotropic hfc A vs O^--Al^{3+} distance (R). Solid line: according to Eq. (10) and Tables I and II. Dotted-dashed line: according to theory assuming $V_{2p_y}=0.368$ H (see text). Experimental data are plotted for R_0, the undistorted O^--Al^{3+} lattice distance. Circle: O^- in Na β-alumina; triangles: O^- in Al_2O_3:Mg^{2+}; cross: $(AlO_4)^0$ in SiO_2; square: $(Al)^0$ in GeO_2.

the R_0 in Table IV and Fig. 6. It turns out, that the O^- site determined in this way is within 0.1 a.u. of the projection of the natural O^- site onto the plane spanned by the three Al^{3+}. Quantitatively, the theory predicts values which are too high by 12—25 %.

Figure 7 shows $B_{\parallel}^D$, $|B_{\parallel}^P|$, and the resulting $B_{\parallel}$ for the parameters given in Tables I and III (solid curves). $B_{\parallel}^P$ follows an exponential law with distance quite well. For distances in the range 3.4 to 4.2 a.u. the calculated $B_{\parallel}$ is practically constant, as is observed experimentally. For very different centers, the observed $B_{\parallel}$ always has approximately the same value, albeit one which is 40—50 % higher than the experimental data. Except for precise agreement, the theory thus predicts satisfactorily the overall observations: (1) A is negative and follows an exponential law with distance and accordingly varies very much from defect to defect. (2) $B_{\parallel}$ is considerably smaller than $B_{\parallel}^D$ and approximately constant over a wide range of O^--Al^{3+} distances.

The quantitative agreement for the undistorted lattices is approximately as good as usually obtained for the theoretical interpretation of hfc's of other point defects in ionic crystals.[15]

For a more detailed quantitative comparison between theory and experiment, which can be useful in applying the theory to estimate lattice expansion or contraction near the defect, one has to discuss two parameters, which enter decisively into the theoretically predicted values: the average excitation energies and the O^--Al^{3+} distances. One would expect the O^--Al^{3+} distance to be somewhat larger than the regular O^{2-}-Al^{3+} distance, since the O^- center is at a positively charged position in the crystal and would tend to repel the Al^{3+} cations. In fact, in previous work the low value of $B_{\parallel}$ compared to $B_{\parallel}^D$ was explained by an increase of that distance of up to ~40%,[3,5] which, as will be shown below, overestimates this effect substantially. The method for determining the electrostatic contribution to the average excitation energies, Eq. (6), on the one hand, probably overestimates the magnitude of this quantity and, on the other hand, does not take into account the crystal-field effects of the surrounding lattice.

From comparing the experimental isotropic hfc's for the unrelaxed O^--Al^{3+} distances with experiment it would appear, that the average electrostatic contribution $V_{2p_y}(2s, 2p_z)$ would be 27% higher than the value corresponding to Eq. (6) (dashed line in Fig. 6). For this value of V_{2p_y}, however, the agreement with the anisotropic hfc's becomes worse. Furthermore, for O^- centers in Na β-alumina the crystal-field energy between p_y and p_z was estimated to be about 10 eV (0.368 H).[1] Taking this value and neglecting the difference between $V_{2p_y}(2p_z)$ and $V_{2p_y}(2s)$ one calculates with Eq. (10) the dotted-dashed line in Fig. 6. The experimental isotropic hfc for Na β-alumina at the regular distance then comes out too high by nearly a factor of 2. This discrepancy can be explained by an increase of 11% in the O^--Al^{3+} distance to $R = 3.52$ a.u. The dotted-dashed curve in Fig. 7 represents $B_{\parallel}$ estimated for this crystal-field energy. $B_{\parallel}$ is smaller for decreasing electrostatic contribution to the excitation
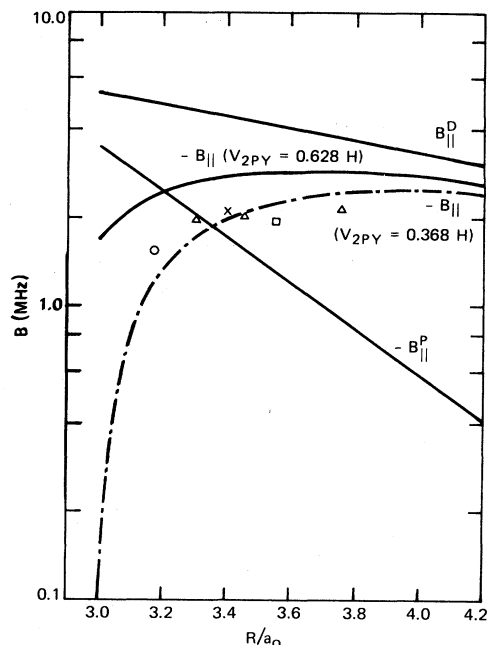

FIG. 7. Semilog plot of the components $B_{\parallel}^D$ and $-B_{\parallel}^P$ of the anisotropic hfc $\beta_{\parallel}$ and of $B_{\parallel}$ vs O^--Al^{3+} distance (R). Solid lines: according to theory and Tables I, III, and IV. Dotted-dashed line: according to theory assuming $V_{2p_y} = 0.368$ H (see text). Experimental data for $B_{\parallel}$ are plotted for R_0, the undistorted O^--Al^{3+} lattice distance. Circle: O^- in Na β-alumina; triangles: O^- in Al_2O_3:Mg^{2+}; cross: $(AlO_4)^0$ in SiO_2; square: $(Al)^0$ in GeO_2.

energy. However, in this case, the theoretical value is still too high by ~30%. To explain the experimental $B_{\parallel}$ value, one would need an increase in distance by only ~5%. It must be added, however, that the estimate for $B_{\parallel}$ is less accurate than for A, since it involves the difference of a number of terms comparable in magnitude which can contribute to a lack of precision.

For $(Al)^0$ centers in GeO_2 the crystal-field energy was estimated to be 0.7 H.[2] Using this as the average V_{2p_y} in Eq. (10), A for the regular distance is only slightly higher than the observed value, and exact agreement requires only a 1% increase in O^--Al^{3+} distance. This very small increase, compared to the former case, is expected, since in this center the charges are reduced by one unit at both O^- and the Al^{3+} which replaces the Ge^{4+} ion, so that one should expect pretty much the perfect crystal bond distance. The value for $B_{\parallel}$ is again too high, here by ~50% (see Table V).

The crystal-field energy at the O^- site in Al_2O_3 for an Al^{3+} vacancy in the second-neighbor shell was calculated to be 15.2 eV (0.559 H).[16,17] If a Mg^{2+} is occupying the Al^{3+} vacancy, it is lowered to 7.7 eV (0.283 H).[17] As done for the previous centers, the isotropic hfc's for R_0 and the increase in O^--Al^{3+} distance necessary to explain the experimental data were calculated for both crystal-field energies (see Table V). Assuming an Al^{3+} vacancy, an increase of R_0 on only 5% is calculated, whereas assuming a Mg^{2+} occupying the Al^{3+} site requires a 13%

increase in R_0 to explain the experimental value. Comparing this with the previous results in GeO_2 and Na β-alumina, one would rather expect an increase of 13% than 5%, since the low value in GeO_2 was due to the fact that no net charge repulsion occurred there contrary to what is expected here. The better agreement for $B_\parallel$ for the Mg^{2+} assumption seems fortuitous. For both models the nearly constant $B_\parallel$ for the three different distant Al^{3+} neighbors is reproduced by the theory. Although one cannot settle beyond doubt for one of the two models from this theoretical estimate, it seems more likely that Mg^{2+} is present in the Al^{3+} vacancy as is also reasonable considering the very large positive Coulomb energy of an Al^{3+} vacancy.

In Al_2O_3, the O^- may not be in the plane spanned by the three Al^{3+} neighbors, since it was observed that the principal z axes of the Al hyperfine tensors do not lie exactly in that plane, which would be expected if it was in the plane. The O^- ion is probably somewhat above the plane towards the O^{2-} lattice site with the p orbital perpendicular to the plane. This introduces also a small positive contribution to the isotropic hfc's due to overlap terms. A more detailed discussion of the hf interactions and the model for this center will be given in Ref. 4.

Finally, the hfc's of $(AlO_4)^0$ centers in SiO_2 seem to fit into the range of values discussed above (see Figs. 6 and 7 and Table V). R_0 in Table V is an estimate of the Al-O bond length in quartz which was obtained by scaling the Si—O long bond length by the ratio of the Al—O and Si—O bond lengths in various oxides.[3] Also for this center one certainly expects an increase of the O^--Al^{3+} distance as in the other centers discussed. Unfortunately, there is no estimate of the crystal field available It is difficult to calculate it because of the more covalent nature of the crystal compared to the other crystals discussed. The values for V_{2p_y} from Table I [Eq. (6)] are approximately an upper limit judging from the experimental isotropic hfc for the nonrelaxed O^--Al^{3+} distance. Taking $V_{2p_y} \approx 10$ eV as an average value between this and no elec-

trostatic contribution at all, which is the unlikely other extreme, one arrives at an increase of the O^--Al^{3+} distance of $\sim 9\%$. This is much smaller than the increase of about 40% estimated previously on the basis of a point-dipole model to explain the anisotropic hfc without considering the polarization effects.[3]

In summary, the theory of transferred spin polarization on the oxygen ion to the neighboring Al^{3+} ions explains the major features of the hfc's in a number of O^--Al^{3+} defects in which Al^{3+} is in a nodal plane of the unpaired oxygen p orbital A rather precise estimate of the O^--Al^{3+} distance can be achieved from the experimental isotropic hfc's when the electrostatic contribution to the average excitation energy of oxygen is approximately known. Since A depends exponentially on this distance, this estimate is rather good despite uncertainties in the average excitation energies. On the other hand, with an estimate of the bond length and the experimental value for the isotropic hfc, one can obtain an approximate crystal-field energy which is often difficult to obtain. The theoretical values for $B_\parallel$ are less reliable since it is the difference of a fairly large number of terms of comparable magnitude. The theory reflects, however, the experimental findings of nearly the same value of $B_\parallel$ for a wide range of O^--Al^{3+} distances and it explains the strong reduction compared to a pure classical dipole-dipole interaction. It was not attempted in this paper to apply the theory to all known O^--Al^{3+} centers. Its application should, however, lead to more reliable estimates of the bond lengths than was possible so far.

[1]R. C. Barklie, J. R. Niklas, J. M. Spaeth, and R. H. Bartram, J. Phys. C **16**, 579 (1983).

[2]M. Stapelbroek, R. H. Bartram, O. R. Gilliam, and D. P. Madacsi, Phys. Rev. B **13**, 1960 (1976).

[3]R. H. Nuttal and J. H. Weil, Can. J. Phys. **59**, 1696 (1981).

[4]R. C. DuVarney, J. R. Niklas, and J. M. Spaeth (unpublished).

[5]M. Stapelbroek, O. R. Gilliam, and R. H. Bartram, Phys. Rev. B **16**, 37 (1977).

[6]R. E. Watson and A. J. Freeman, *Hyperfine Interactions* (Academic, New York, 1967), pp. 53—94.

[7]D. Ikenberry, B. K. Rao, S. D. Mahanti, and T. P. Das, J. Magn. Reson. **1**, 221 (1969).

[8]D. Ikenberry, A. N. Jette, and T. P. Das, Phys. Rev. B **1**, 2785 (1970).

[9]D. Ikenberry and T. P. Das, Phys. Rev. B **2**, 1219 (1970).

[10]O. F. Schirmer, J. Phys. C **6**, 300 (1973).

[11]F. J. Adrian and A. N. Jette, J. Chem. Phys. **81**, 2415 (1984).

[12]E. Clementi and C. Roetti, At. Data Nucl. Data Tables **14**, 177 (1974).

[13]R. T. Cox, Solid State Commun. **9**, 1989 (1971).

[14]R. H. Bartram, C. E. Swenberg, and J. T. Fournier, Phys. Rev. **139**, A941 (1965).

[15]A. M. Stoneham, *Theory of Point Defects* (Oxford University Press, New York, 1975).

[16]S. Y. La, R. H. Bartram, and R. T. Cox, J. Phys. Chem. Sol. **34**, 1079 (1973).

[17]R. H. Bartram (private communication).